

DESIGN OPTIMIZATION OF JT-60SU FOR STEADY-STATE ADVANCED OPERATION

K. USHIGUSA, G. KURITA, N. TOYOSHIMA, K. NAGASHIMA, Y. NEYATANI, N. MIYA, S. ISHIYAMA, M. KIKUCHI, A. ISAYAMA, S. ISHIDA, H. SHIRAI, M. KURIYAMA, T. ITOH, T. YAMAMOTO, Y. IKEDA, T. IMAI, K. HAMAMATSU, K. TOBITA, M. MATSUKAWA, H. KUBO, S. NAKAGAWA, K. MORI, T. KITAI, S. OGURI, M. OTSUKA¹⁾, K. NAKASHIMA²⁾, S. NAKAGAWA³⁾, R. STAMBAUGH⁴⁾, D.L. SEVIER⁴⁾, M. NAGAMI, H. NINOMIYA, M. AZUMI, H. KISHIMOTO

Japan Atomic Energy Research Institute,
Naka Fusion Research Establishment
Naka-machi, Naka-gun, Ibaraki-ken, 311-0193 Japan

- ¹⁾ Hitachi limited, Hitachi-shi, Ibaraki-ken Japan
²⁾ Mitsubishi Fusion Center, Chiyoda-ku, Tokyo, Japan
³⁾ Toshiba Corporation, Chiyoda-ku, Tokyo, Japan
⁴⁾ General Atomics, San Diego, CA, USA.

Abstract

Design optimization of JT-60SU has been done for a steady-state advanced operation. A transport code simulation indicates that a fully non-inductive reversed shear plasmas with fractions of 70% of the bootstrap current and ~30% of beam driven current can be sustained for more than 1,000s without any additional control. Investigations have been progressed on MHD stability, vertical positional stability and dynamics of the vertical displacement events. Significant progress has been achieved in the R&D of Nb₃Al superconducting wires, low induced activation material (Fe-Cr-Mn steel). A design improvement has been made in TF coils to reduce a local stress on radial disk. Dynamic behaviors of the tokamak machine have been analyzed at emergency events such as an earthquake.

1. INTRODUCTION

The objective of the JT-60 Super Upgrade[1-2] is to establish an integrated physics and technology basis for a steady-state tokamak fusion reactor such as SSTR[3] and for a reduced size of ITER. Important roles of JT-60SU in the world-wide fusion research activities including ITER project are placed on to pioneer in the advanced physics, to develop advanced materials for a tokamak fusion reactor and to establish new technologies for improving reactor operation and maintenance. The machine parameters of JT-60SU are shown in Table I. The machine has been designed to be able to perform DT operation at a certain level by adding extra radiation shield and the isotopic separation system. A fully non-inductive discharge based on ELMy H-mode at the plasma current of ~5MA and the average density of $\sim 0.88 \times 10^{20} \text{m}^{-3}$ with 60MW of CD power is the first candidate as a steady-state operation scenario in JT-60SU. This paper describes another advanced steady-state operation scenario based on the reversed magnetic shear configuration. This paper emphasizes a recent progress on R&D of Nb₃Al superconducting wires and a low induced activation material for JT-60SU. Robustness of the machine against an emergency event such as an earthquake is studied also.

2. OPTIMIZATION OF STEADY-STATE OPERATION SCENARIO

2.1 Transport simulation for the advanced steady-state operation scenario

A high fusion performance with a reversed magnetic shear plasma has been obtained in recent JT-60 experiments[4,5], where the equivalent $Q_{DT}=1.25$ has been transiently achieved. Sustainment of reversed shear with the internal transport barrier (ITB) was also demonstrated by current profile control in JT-60U[6]. On the based of the JT-60 result, a transport code simulation taking into account a reduction of the thermal diffusivity near the location of minimum safety factor has been performed to find out the optimum operation scenario to produce and to sustain the reversed shear configuration in JT-60SU. Numerical simulation is performed by using 1.5D transport code system

TOPICS[7]. In order to simulate reversed field plasmas observed in JT-60U, following transport coefficients are assumed:

$$\begin{aligned} \chi_{e/i} &= \chi_{e/i}^{\text{ano}} + C_{e/i} \chi_{e/i}^{\text{NC}} \\ \chi_{e/i}^{\text{ano}} &= C_{e/i1} (1 + C_{e/i2} a^2)^{-1} \frac{a^2}{\tau_{85\% \text{ELMfree}}} E_{e/i}(s) \\ E_{e/i}(s) &= \left[1 + \exp \left\{ \frac{E_{e/i}(s)}{\chi_{e/i}} \right\} \right]^{-1} + \left[1 + \exp \left\{ - \frac{E_{e/i}(s)}{\chi_{e/i}} \right\} \right]^{-1} \\ D &= C_d \chi_{e/i} \end{aligned}$$

where $\chi_{e/i}$ and $\chi_{e/i}^{\text{NC}}$ are the electron/ion thermal diffusivity and the ion neo-classical diffusivity,

operation parameters	DD	DT	DT
plasma current I_p (MA)	5	10	6.2
toroidal field B (T)	6.25	6.0	5.77
major radius R_p (m)	4.8	5.0	5.2
minor radius a_p (m)	1.3	1.5	1.35
ellipticity	1.8	1.8	1.8
triangularity	0.4	0.4	0.4
safety factor q_5	6.2	3.8	4.5
density $\langle n_e \rangle$ (10^{19} m^{-3})	8.8	10.0	8.4
-particle fraction	----	----	0.05
beam power P_{NB} (MW)	60	60	50
fusion gain Q_{DT}	----	----	5.0
confinement time τ_E (s)	1.54	3.24	1.71
beta (%)	1.24	1.83	2.39
normalized beta β_N	2.01	1.65	3.0
poloidal beta β_p	1.73	0.79	2.0
bootstrap current I_{BS}/I_p	0.50	0.23	0.51
beam driven current I_{BD}/I_p	0.50	0.22	0.49

TABLE I Standard Operation Parameter in JT-60SU

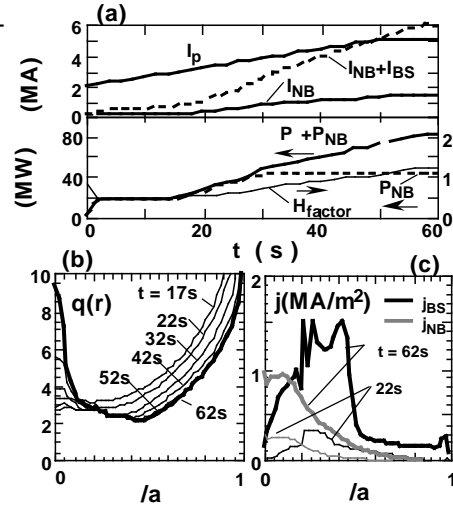


Fig.1 Current ramp-up scenario for reversed shear formation in JT-60SU

$s(=r(dq/dr)/q)$ is the magnetic shear, a is the minor radius, and $C_{e/i1}$, $C_{e/i2}$, $C_{e/iNC}$, $\chi_{e/i}$, $\chi_{e/i}^{\text{NC}}$ are constant. The quantity $\tau_{85\% \text{ELMfree}}$ is the confinement time of 85% ELMFree scaling. The function $E(s)$ varies from 1 to 0 with a typical width on s of $\sim \chi_{e/i}$, and connects transport with the current profile. We assume that $E(s) = 1$ at $|a/a_p| < 0.2$ to fit JT-60U results. Constant $C_{e/i1}$ are selected so that the global energy confinement time becomes reasonable value compared with the 85% ELMFree scaling. To reproduce a similar plasma profile with JT-60 results, constant $C_{e/i2}$ and $C_{e/iNC}$ are set to be 4 and 1 respectively. Following constants are employed in this simulation; $\chi_{e/i} = 5.0$, $\chi_{e/i}^{\text{NC}} = 1.0$, $C_d = 0.1$. Power deposition of neutral beams is calculated by the Fokker-Planck code and the neutral beam driven current is calculated from a simple modeling shown in Ref. [8].

Typical example of reversed shear formation in JT-60SU is shown in Fig.1 where DT plasma is assumed. During a slow current ramp-up phase ($dI_p/dt = 0.06 \text{ MA/s}$), N-NB power with the beam energy of 750keV is injected which drive the current at central region. The NB power is increased during current ramp-up phase up to 40MW (thermalized power). We assumed that ITB is formed at $P_{\text{abs}} > 25 \text{ MW}$. Reversed shear configuration and ITB are formed at $t \sim 22 \text{ s}$ as shown in Fig.1(b). Locations of ITB and q_{min} shift gradually outward due to the increase in the plasma current and bootstrap current. A very large bootstrap current appears at $|a/a_p| = 0.2-0.5$ while N-NB drives a center peaked current as shown in Fig.1(c). At the current flat top ($t = 50 \text{ s}$), the non-inductive current ($I_{\text{NB}} + I_{\text{BS}}$) exceeds the plasma current and the reversed OH current appears at the plasma center. It should be emphasized that the reversed shear profile could be produced by a strong central heating and current drive even in the condition of slow current ramp-up rate.

Time evolution of plasma parameter after the current flat top is shown in Fig. 2(a). The non-inductive current $I_{\text{CD}} (= I_{\text{NB}} + I_{\text{BS}})$ is very close to the plasma current and keeps almost constant under the condition of high bootstrap current fraction ($I_{\text{BS}}/I_p = 70\%$ and $I_{\text{NB}}/I_p = 30\%$). The heating power is $\sim 34 \text{ MW}$ while the NB thermalized power is $\sim 42 \text{ MW}$ ($Q_{\text{DT}} \sim 4$). The thermal energy confinement time is $\sim 1.4 \text{ s}$ and the H-factor ($\tau_E^{\text{th}} / \tau_{85\% \text{ELMfree}}$) is ~ 1.2 . The toroidal beta value is around 1.54% which corresponds to the normalized beta value of $\beta_N = 2.5$. Although the total non-inductive current decreases very slowly ($dI_{\text{CD}}/dt = -0.2 \text{ A/s}$), this reversed shear plasma can be maintained for a long time enough to study characteristic of steady-state plasma performance without any specific

control. A reversed shear plasma with an ITB located outer than this calculation can be also possible in this scheme, however, too high H-factor appears in such condition.

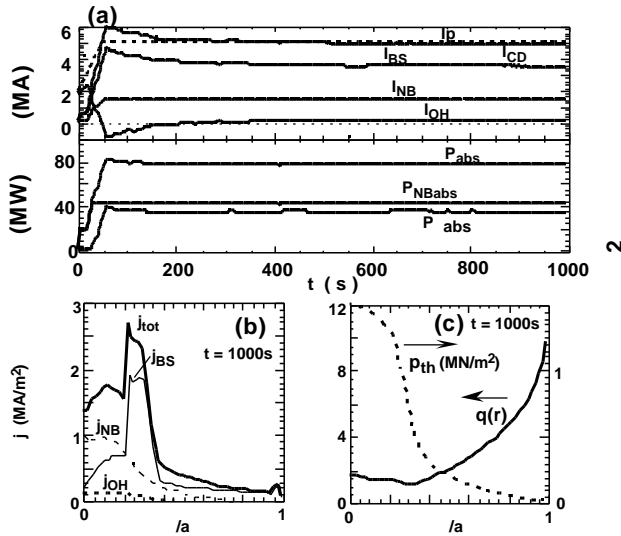


Fig.2 Sustainment of reversed shear non-inductive plasma by N-NBCD alone.

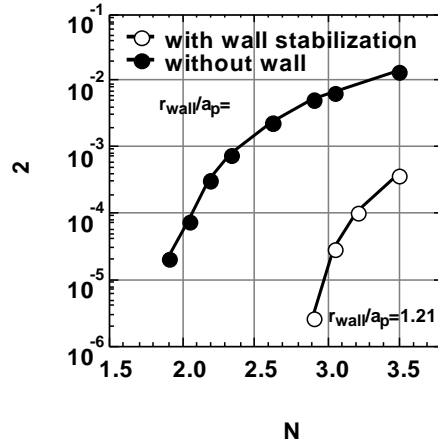


Fig.3 Growth rate of n=1 ideal mode in reversed shear plasmas

2.2 MHD Stability in reversed shear plasmas

In a framework of the previous transport code analysis, a fully non-inductive steady-state operation with a high bootstrap current fraction can be expected in JT-60SU. However, a steep pressure gradient appears at around the radius of q_{min} , and the normalized beta value β_N becomes 2.5. In JT-60U experiment, a high performance discharge in reversed shear plasmas is limited at $\beta_N < 2.3$ [5]. Therefore, the remained critical issue of the advanced steady-state operation in JT-60SU is the MHD stability. In order to check the stability margin the advanced steady-state scenario, the ideal stability of the reversed shear scenario on JT-60SU is investigated using ERATO-J code where similar pressure and current profiles with results in Sec 2.1 are assumed. Stability analysis has indicated that $m=2, n=1$ mode is the most unstable mode. The growth rate of $n=1$ ideal global mode is plotted against β_N in Fig. 3 (solid circles), indicating $n=1$ mode becomes unstable suddenly at around $\beta_N = 2$. In JT-60SU, a low resistivity wall is employed to improve the vertical stability as described in Sec. 2.3. For the ideal MHD stability, the wall stabilization effect can be expected also. ERATO-J code has suggested that the wall stabilization effect enlarges the stable regime up to around $\beta_N \sim 2.8$ with the ideal wall at $r_{wall}/a_p = 1.21$. Further studies including wall stabilizing effect under the realistic wall and optimization on profiles have to be made to enlarge stable regime in advanced high β_N operation.

2.3 Vertical Stability Analysis

Since a highly elongated plasma configuration is employed to realize high current discharge with a limited size of machine in JT-60SU, the vertical instability is also one of key issues to be solved for a stable operation. In JT-60SU, a toroidally continuous divertor baffle plate is employed for improving the passive stabilizing effect of the vacuum vessel. The investigation of n -index, the shell stabilizing index for the JT-60SU equilibrium has shown that the growth rate of vertical stability for an elongated JT-60SU plasmas can be reduced to be less than 30-50Hz by employing the baffle plate[9]. Furthermore, it is found that the vertical positional instability is improved by increasing the triangularity in JT-60SU machine. Dynamic analysis of the vertical displacement event(VDE) has been performed by using Toroidally Symmetric Plasma Simulation (TSPS) code in which Grad-Shafranov equation and linearized equations of plasma motion taking into account the effects of eddy current on the vessel and baffle plates are iteratively solved[10]. Fast vertical position control by two sets of normal conductors(10 turns) located near the vacuum vessel is taken into account in this simulation. Dynamic analysis has indicated that VDE can be suppressed by the fast feedback control with the designed power supply voltage (200V) for minor disruptions with a rapid decrease in β_p ($|\beta_p| < 0.6$ for 10ms). Combination of improvement of passive stabilizing effect by divertor baffle plate and the fast position feedback control system has made an enough

stability margin for the vertical positional instability in JT-60SU.

3. PROGRESS ON MACHINE DESIGN

As a superconducting wire for toroidal field magnets, Nb₃Al conductor is adopted in JT-60SU. Nb₃Al as a high field superconducting wire has a much better J_c property against a strain on the conductor than Nb₃Sn. Through R&D of Nb₃Al strand satisfying JT-60SU design condition, almost all important engineering techniques for manufacturing Nb₃Al strand for JT-60SU is established. By connecting two adjacent TF coils with shear panel, a large magnetic energy (~24G) can be stored by a light coil system(~3000tons including shear panel) with a small coil displacement (11mm). However, the maximum local stress of 750MPa was found in detail FEM analysis[4]. By increasing the length of the wedge part of coil case, the maximum local stress is reduced to 643MPa which satisfies the acceptable limit (667MPa). The first candidate for material of the vacuum vessel in JT-60SU is a low cobalt 316SS (0.05% Co) and the inner surface is covered by W shield(3cm). Fe-Cr-Mn steels(C:0.02-0.2wt%, Mn:15wt%, Cr:15-16wt%, N:0.2wt%), which has a lower induced-radio-activity than 316SS, has been developed as another material of structure components for JT-60SU[11]. It has been confirmed that the developed high manganese steels have excellent mechanical properties and high resistance within standard temperature of JT-60SU vacuum vessel. By using this steel as the vacuum vessel, a rapid decay of the radioactivity of the machine than 316SS can be realized after two years DT operation.

JT-60SU superconducting coil systems (TF:2340tons, EF:520tons, shear panels:660tons and CS is not included) are modeled to analyze their dynamic behaviors during an earthquake. Fundamental frequency of vibration in JT-60SU coil systems is 10.3Hz and larger than that of ITER(1.5Hz[12]). It is found that a weight reduced design of TF coils, shear panel connection and favorable design of supporting system contribute to realize a higher fundamental frequency for vibration. With the acceleration (350-400gal) of the basement of the machine room calculated from EL Centro and TAFT wave forms analysis has indicated that the maximum displacement of the TF coil is within 2mm. Vibration analysis of the vacuum vessel is also performed by the response spectrum analysis method. A fundamental frequency for the vibration is 6.1Hz and maximum displacement is within 2.3mm at the same acceleration described above. From these analyses, an enough robustness of JT-60SU system against an earthquake has been confirmed.

ACKNOWLEDGMENTS

The authors would like to acknowledge JT-60 Team, JAERI Tritium Process Laboratory, JAERI Superconducting Magnet Laboratory, Hitachi Cable Limited, Showa W.C.C, and Sumitotmo E.I..

REFERENCES

- [1] NINOMIYA, H., et al., in Plasma Phys. Contr. Nucl. Fusion Res. (Seville), vol.2, (1995) 613.
- [2] KIKUCHI, M., et al., in Fusion Energy Conf. 1996 (Montreal 1996), vol.3, (1997) 451.
- [3] SEKI, Y., et al., in Plasma Phys. Contr. Nucl. Fusion Res., vol.3, (1990) 473.
- [4] ISHIDA, S., et al., in Fusion Energy Conference 1998 (Yokohama), IAEA-F1-CN-69/OV1-1.
- [5] FUJITA, T., et al., in Fusion Energy Conference 1998 (Yokohama), IAEA-F1-CN-69/EX1-2.
- [6] IDE, S., et al., in Fusion Energy Conference 1998 (Yokohama), IAEA-F1-CN-69/CD1-4.
- [7] Annual Report of the Naka Fusion Research Establishment for the period of April 1990 to March 31 1991, Rep. JAERI-M-91-159, Japan Atomic Energy Research Institute(1991)59.
- [8] MIKKELSEN, D.R. et al., Nuclear Tech./Fusion 4(1983)237.
- [9] KURITA, G., et al., Fusion Eng. Design 38(1998)417.
- [10] SENDA, I., et al., JAERI-Data/Code 95-010, Internal Report of JAERI, 1995.
- [11] ISHIYAMA, S., et al., to be published in J. of Nuclear Materials.
- [12] Technical Basis of the ITER Final Design Report (1997), Chapter IV, p.46.